


Hippocampal synaptic and neural network deficits in young mice carrying the human *APOE4* gene

Guo-Zhu Sun^{1,2} | Yong-Chang He^{1,2} | Xiao Kuang Ma^{2,3,4} | Shuang-Tao Li^{2,3} |
De-Jie Chen² | Ming Gao² | Shen-Feng Qiu⁴ | Jun-Xiang Yin⁵ | Jiong Shi^{5,6} | Jie Wu^{2,3,4} 

¹Department of Neurosurgery, The Second Hospital of Hebei Medical University, Shijiazhuang, Hebei, China

²Department of Neurobiology, Barrow Neurological Institute, St. Joseph's Hospital and Medical Center, Phoenix, AZ, USA

³Department of Physiology, Shantou University Medical College, Shantou, Guangdong, China

⁴Department of Basic Medical Sciences, University of Arizona College of Medicine, Phoenix, AZ, USA

⁵Department of Neurology, Barrow Neurological Institute, St. Joseph's Hospital and Medical Center, Phoenix, AZ, USA

⁶Department of Neurology, Tianjin Neurological Institute, Tianjin Medical University General Hospital, Tianjin, China

Correspondence

Jie Wu, Department of Neurobiology, Barrow Neurological Institute, St. Joseph's Hospital and Medical Center, Phoenix, AZ, USA.
Email: jie.wu@dignityhealth.org

Funding information

Arizona Alzheimer's Disease Consortium; Barrow Neurological Foundation; the National Science Foundation of China, Grant/Award Number: 81671050; the Program for High-level Talent Fund of Hebei Province of China, Grant/Award Number: A201401041 to GS

Summary

Introduction: Apolipoprotein E4 (*APOE4*) is a major genetic risk factor for late-onset sporadic Alzheimer disease. Emerging evidence demonstrates a hippocampus-associated learning and memory deficit in aged *APOE4* human carriers and also in aged mice carrying human *APOE4* gene. This suggests that either exogenous *APOE4* or endogenous *APOE4* alters the cognitive profile and hippocampal structure and function. However, little is known regarding how *Apoe4* modulates hippocampal dendritic morphology, synaptic function, and neural network activity in young mice.

Aim: In this study, we compared hippocampal dendritic and spine morphology and synaptic function of young (4 months) mice with transgenic expression of the human *APOE4* and *APOE3* genes.

Methods: Hippocampal dendritic and spine morphology and synaptic function were assessed by neuronal imaging and electrophysiological approaches.

Results: Morphology results showed that shortened dendritic length and reduced spine density occurred at hippocampal CA1 neurons in *Apoe4* mice compared to *Apoe3* mice. Electrophysiological results demonstrated that in the hippocampal CA3-CA1 synapses of young *Apoe4* mice, basic synaptic transmission, and paired-pulse facilitation were enhanced but long-term potentiation and carbachol-induced hippocampal theta oscillations were impaired compared to young *Apoe3* mice. However, both *Apoe* genotypes responded similarly to persistent stimulations (4, 10, and 40 Hz for 4 seconds).

Conclusion: Our results suggest significant alterations in hippocampal dendritic structure and synaptic function in *Apoe4* mice, even at an early age.

KEYWORDS

apolipoprotein E4, dendrites, hippocampus, synaptic plasticity, theta oscillations

1 | INTRODUCTION

Alzheimer disease (AD) is a neurodegenerative disorder characterized by progressive learning and memory deficits. Amyloid plaques, neurofibrillary tangles, and neocortical synaptic loss contribute to AD

pathogenesis.¹⁻⁶ The advent of molecular imaging techniques and biomarker studies has demonstrated that in AD patients, pathologic changes occur a couple of decades earlier than the onset of clinical symptoms.⁷⁻¹³ It is well accepted that synaptic dysfunction and loss are early changes in AD pathogenesis.¹⁴⁻¹⁶ The synaptic abnormalities are particularly pronounced in the hippocampus, which underlies cognitive deficits in the early stage of developing AD.

Jiong Shi and Jie Wu played an equal role as senior authors in this article.

Of the three alleles of human apolipoprotein E (APOE2, 3, and 4), APOE4 is the major genetic risk factor for late-onset sporadic AD.¹⁷⁻²² Accumulating evidence demonstrates that APOE4 is associated with increased deposition of amyloid- β ,^{23,24} hyperphosphorylation of tau,^{25,26} altered synaptic morphology,²⁷⁻²⁹ impaired neuronal plasticity,³⁰⁻³³ and declining memory.^{34,35} Either exogenous APOE4 or endogenous APOE4 alters the cognitive profile and hippocampal structures and functions, which underlies synaptic impairment and learning and memory deficits in AD. In a large study of 815 subjects with normal cognitive status (317 APOE4 carriers and 498 noncarriers), APOE4 carriers showed a longitudinal decline in memory that began before the age of 60 years, and they had greater acceleration in cognitive decline than noncarriers.³⁶ In another study of healthy infant carriers and noncarriers of APOE4, infant APOE4 carriers had lower white matter myelin and gray matter volume in brain areas that are vulnerable in AD, such as the precuneus, posterior/middle cingulate, and lateral temporal. This indicates the impact of APOE4 at the earliest stage of brain development.³⁷ APOE4 likely affects hippocampal structure and function.³³ Both hippocampal synaptic morphology and hippocampus-associated learning behavior alterations have been found in young (4-month-old) *Apoe4* transgenic mice (*Apoe4* mice).^{38,39} Interestingly, these synaptic pathologic changes are associated with an accumulation of amyloid β 42 and hyperphosphorylated tau and reduced levels of vesicular glutamate transporters in hippocampal neurons. Electrophysiological studies demonstrated the impairment of hippocampal synaptic plasticity (long-term potentiation, LTP) in aged *Apoe4* mice using in vitro hippocampal slices⁴⁰ and in wild-type mice with local injection of *Apoe4*.⁴¹ However, the alterations in synaptic functions in young *Apoe* mice remain unclear. Both enhancements⁴² and no change³² of hippocampal synaptic LTP have been reported in young *Apoe4* mice compared to *Apoe3* mice. Although 4-month-old *Apoe4* mice have shown hippocampal synaptic morphological changes and hippocampus-associated learning behavioral decline,^{38,39,43,44} the hippocampal synaptic function in these young *Apoe4* mice has not been studied. In the present study, we profiled hippocampal dendritic and spine morphology in *Apoe4* and *Apoe3* mice; evaluated the roles of *Apoe4* in hippocampal synaptic function including synaptic transmission, paired-pulse facilitation (PPF), and LTP; examined hippocampal theta oscillations and synaptic responses to sustained stimuli with different frequencies using 4-month-old *Apoe4* mice; and compared these results to age-matched *Apoe3* mice. Our results demonstrate the alterations in hippocampal synaptic morphology, function, and neuronal network synchronization in young *Apoe4* mice.

2 | METHODS

All experimental protocols were approved by and performed in accordance with guidelines set by the animal care and use and ethical committees at the Barrow Neurological Institute, Hebei Medical University (Shijiazhuang, Hebei, China) and Shantou University Medical College (Shantou, Guangdong, China).

2.1 | Hippocampal slice preparation

Hippocampal slices were prepared from 4- and 12-month-old male mice. *Apoe4* mice were generated as described previously.⁴⁵ *Apoe3* mice were used as controls. Briefly, *Apoe* transgenic mice were generated using a microinjection of allele-specific human E3 or E4 genomic fragments to establish founders. The founders were then bred to *Apoe* knockout mice lacking a functional mouse *Apoe* protein. These transgenic lines transcribe and express appropriate human APOE3 and APOE4 proteins in brain, liver, and other tissues without contamination of the endogenous mouse *Apoe* gene. Under isoflurane anesthesia, mice were sacrificed in accordance with Barrow Neurological Institute's Institutional Animal Welfare Committee guidelines, as described previously.⁴⁶⁻⁴⁸ Brain tissue was quickly removed and bathed in cold (4°C) artificial cerebrospinal fluid (ACSF) containing (in m mol L⁻¹): NaCl, 119; KCl, 2.5; NaHCO₃, 26; MgSO₂, 1.3; NaH₂PO₄, 1.0; CaCl₂, 2.5; and glucose, 11. The ACSF was continuously bubbled with 95% O₂-5% CO₂ (carbogen). Several coronal sections (400 μ m thick) containing the dorsal hippocampus were cut using a vibratome (Vibratome 1000 Plus, The Vibratome Company, St. Louis, MO, USA) and incubated at room temperature (21 \pm 1°C) for at least 60 minutes prior to recording. Thereafter, one slice was transferred to a liquid-air interface chamber (Warner Instrument, LLC, Hamden, CT, USA) and suspended on nylon net in a bath of continuously dripping oxygenated ACSF (2.0 to 2.5 mL/min). Humidified carbogen was passed along the upper surface of the slice, and bath temperature was regulated by a feedback circuit accurate to 31 \pm 0.5°C. Baseline temperature was 30 \pm 1°C.

2.2 | Electrophysiological recordings

Standard field potential recordings were performed on the hippocampal CA1 region using borosilicate glass micropipettes pulled to a tip diameter of about 1 μ m and filled with 2 mol L⁻¹ NaCl.⁴⁶⁻⁴⁸ To record synaptic potentials, a recording electrode was placed at the CA1 apical dendrite region. Stimulus intensity was set based upon input-output relationships and was 50% of the maximal response. For testing PPF, two stimuli with 50% of the maximal intensity were given at 15-, 50-, 100-, and 400-ms intervals. For recording LTP, stable baseline synaptic potentials (50% of the maximal intensity) were recorded for 20 minutes, and then a theta-burst tetanic stimulation that contained 15 burst trains at 5 Hz was delivered (each train contained five pulses at 100 Hz). Thereafter, the baseline intensity-evoked field excitatory post-synaptic potentials (fEPSPs) were recorded for 60 minutes with 0.33 Hz. A custom bipolar platinum wire electrode (0.08 mm diameter) was placed at the Schaffer collateral pathway, and stimulation was delivered using a Model 2100 A-M Systems Isolated Pulse Stimulator (Carlsborg, WA, USA). All evoked responses were recorded using an Axoclamp-2B amplifier, and data acquisition was controlled by pClamp 10.2 software (Molecular Devices, Sunnyvale, CA, USA).

2.3 | CA1 neuron morphology quantification

In experiments where quantification of CA1 neuronal morphology was desired, we included 0.25% biocytin in a K^+ -based internal electrode solution and dialyzed the neurons in acute slices for 10 minutes (500 pA current injection). The slices were then fixed in 4% paraformaldehyde overnight, permeabilized with 0.2% Triton X-100, followed by a 48-hours incubation with avidin-Alexa Fluor 488 (Invitrogen, Carlsbad, CA, USA). The dendritic arbor was traced into a three-dimensional structure using NeuroLucida (MicroBrightField, Williston, VT, USA), as described previously.⁴⁹ Neurons were coded for blinded analysis. Dendritic measures including branch number, pattern, and total dendritic length were analyzed using NeuroLucida Explorer. In addition, Sholl analyses⁵⁰ were performed in these reconstructed neurons to extract morphometric parameters on regional alterations in the dendritic arbor structure, including dendritic length, branching complexity, and branch point locations within a series of concentric circles (20 μm radius increment from soma) on the entire dendritic arbors. At least three mice were reconstructed for each genotype group.

For dendritic spine analysis, we used Imaris software (version 8.02, 64 bit; Bitplane) on collected confocal Z-stack images.⁴⁹ We selected secondary apical dendritic branches that were located at 100–200 μm from the soma for analysis. At least two dendritic segments were quantified per neuron. Image Z-stacks were acquired using a Zeiss confocal microscope (LSM 710, with 63 \times NA 1.4 oil-immersion objective, 0.2 μm Z resolution). The confocal files were imported into Imaris software, and the Filament Tracer module was used for three-dimensional rendering of each dendritic segment. Reconstructed spines were subsequently edited manually to exclude spines that were misidentified. Spine parameters, including density, head size, and head volume, were quantified. At least 250 spines from three mice were constructed for each group.

2.4 | Data acquisition and analysis

Electrophysiological data were acquired by pClamp 10.2 via an Axon Digidata 1550A (Molecular Devices) interface board set to a sampling frequency of 10 kHz, filtered in Clampfit 10.2 using an

eight-pole Bessel filter and a 1-kHz low-pass filter, and stored on hard media for subsequent off-line analysis. Statistical comparisons of results were performed using Origin 8.0 (Microcal Software, Northampton, MA, USA). The Student *t* test, one-way or two-way (Sholl analyses of dendritic length and intersection numbers) analysis of variance was used when data passed normality tests. For dendritic spine volume tests, a nonparametric Mann-Whitney *U* test was used. Statistical difference was assessed, and $P < .05$ was set as the level of significance.

3 | RESULTS

3.1 | Hippocampal neuronal dendritic and spine comparisons between young *ApoE3* and *ApoE4* mice

To compare the dendritic length and spine density of hippocampal CA1 neurons, we added biocytin into the recording solution and dialyzed the CA1 pyramidal neuron under the patch-clamp whole-cell recording in current-clamp mode. We then reconstructed these labeled neurons for quantitative analysis (Figure 1A,B). As shown in Figure 2A,B, the dendritic length and the numbers of intersections of the dendritic arbor in *ApoE4*-mouse CA1 neurons compared to those from *ApoE3*-mouse neurons) were significantly reduced (genotype effects for dendritic length: $F_{(1,187)} = 20.54$, $P < .001$; number of intersections: $F_{(1,160)} = 9.49$, $P = .002$). To analyze hippocampal CA1 neuron spine morphology, we used Imaris reconstruction from confocal Z-stack images (see Figure 1). Quantitative analysis revealed that *ApoE4* neurons exhibited significantly reduced spine head volume compared to *ApoE3* neurons (Figure 2C, $P < .01$, Mann-Whitney *U* test). Spine density in *ApoE4* neurons ($n = 7$) was also significantly lower than in *ApoE3* neurons ($n = 8$, Figure 2D; 10.3 ± 0.33 spines per 10 μm dendrite in *ApoE4* neurons compared with 13.2 ± 0.9 in *ApoE3* neurons; $P < 0.01$, unpaired *t* test). These morphology results indicate that hippocampal CA1 neurons in young *ApoE4* mice have reduced dendritic length, spine size, and density compared with the *ApoE3* controls. Considering that spine size and geometry are highly correlated with glutamatergic synapse function,⁵¹ these results suggest potentially altered hippocampal synaptic function in young *ApoE4* mice.

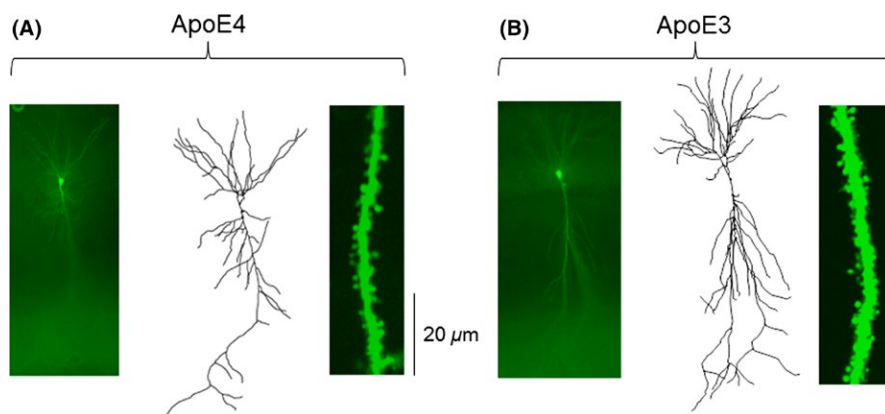


FIGURE 1 Comparison of dendritic length and spine density between *ApoE4* (A) and *ApoE3* (B) transgenic mice. Photomicrographs of biocytin-stained hippocampal CA1 pyramidal neurons are shown in the left panels, representative dendritic arbor reconstructions using NeuroLucida are shown in the middle panels, and dendritic segments from which dendritic spine density was calculated are shown in the right panels

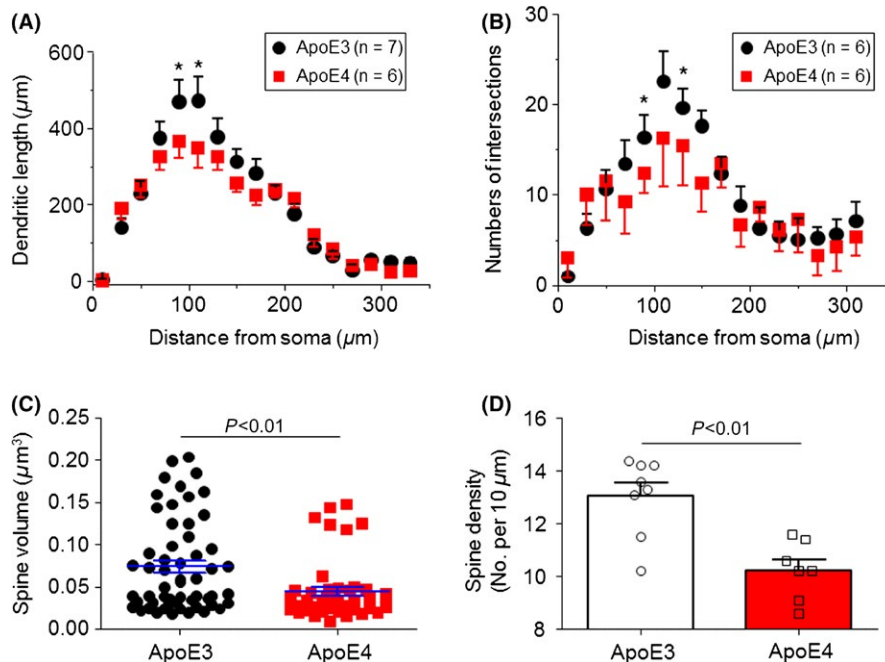


FIGURE 2 Quantitative analysis of dendritic complexity and spine size and density in *ApoE3* and *ApoE4* mice. Sholl analysis of hippocampal CA1 neuron dendritic complexity shows a significant reduction in dendritic length (A) and intersection numbers (B) (* $P < .05$, t test). Further analysis shows a significant reduction in spine volume (C) and density (D) in *ApoE4* compared to *ApoE3* mice

3.2 | Input-output relationships in hippocampal slices prepared from young *ApoE4* and *ApoE3* mice

We next compared input-output relationship curves between hippocampal slices prepared from 4-month-old *ApoE4* and *ApoE3* mice. Repetitive stimulation (0.33 Hz) of Schaffer collaterals evoked fEPSPs in the hippocampal CA1 region (Figure 3A). In both *ApoE3* and *ApoE4* groups, hippocampal slices were stimulated with different intensities (from 2 to 10 V at intervals of 33 seconds with the stimulation pulse duration of 0.1 ms), and these stimuli induced increases in the slope of the fEPSPs, which were plotted against stimulation intensities to form an input-output relationship curve (Figure 3B). Because the input-output curves between 4 and 10 V were linear, we fitted each individual slice (between 4 and 10 V) using a linear equation and compared the linear slopes of input-output relationships between the *ApoE3* and *ApoE4* groups. As shown in Figure 3C, the linear slope for the *ApoE3* group was 0.49 ± 0.04 mV/ms, while that for the *ApoE4* group was 0.89 ± 0.08 mV/ms. Statistical analyses revealed a significant difference between these two groups ($P < .0001$, unpaired t test). These results suggest that compared to *ApoE3* control mice, *ApoE4* transgenic mouse hippocampal CA1 neurons exhibit an enhanced excitability.

3.3 | Paired-pulse facilitation in hippocampal slices prepared from young *ApoE4* and *ApoE3* mice

To measure synaptic short-term plasticity, we used a PPF protocol in hippocampal slices from 4-month-old *ApoE4* and *ApoE3* mice. It has been reported that stimulus-evoked response to a second stimulation is potentiated if it is delivered within 200 ms of the first stimulus.⁵² In these experiments, we measured PPF using interpulse intervals of 15, 50, 100, and 400 ms. Figure 4A shows the typical

traces of PPF with a 50-ms interpulse interval in *ApoE3* and *ApoE4* hippocampal slices. Statistical analysis from 54 total slices (30 from *ApoE4* mice and 24 from *ApoE3* mice) demonstrated a significant enhancement of the ratio of P2/P1 at all tested P1 and P2 intervals in *ApoE4* mice compared to *ApoE3* mice (Figure 4B), suggesting an enhanced hippocampal synaptic short-term plasticity in young *ApoE4* mice.

3.4 | Long-term potentiation in hippocampal slices prepared from young *ApoE4* and *ApoE3* mice

To compare hippocampal CA1 synaptic LTP between *ApoE4* and *ApoE3* mice, we measured the theta-burst stimuli-induced LTP in the hippocampal Schaffer collateral-CA1 pathway. The theta-burst stimulation contained five trains with intervals of 10 ms (100 Hz), 10 times at 100-ms intervals. For LTP recordings, baseline fEPSPs (50% of maximal stimuli with 0.33 Hz) were recorded for 20–30 minutes. If the variation in the baseline was within $\pm 10\%$, theta-burst tetanic stimuli were delivered. Thereafter, baseline stimulus-induced fEPSPs were recorded for 60 minutes (Figure 5A). Plot recording time to normalized fEPSP slopes (baseline level as 1) from pooled data showed an impaired LTP induction (after theta-burst stimulation 0–10 minutes) and maintenance (after theta-burst stimulation 50–60 minutes) in the *ApoE4* group compared to *ApoE3* mice (Figure 5B). Statistical analysis showed that the mean LTP induction in the *ApoE4* group was 1.38 ± 0.02 and 1.52 ± 0.02 in the *ApoE3* group ($P < .001$, unpaired t test); mean LTP maintenance in the *ApoE4* group was 1.31 ± 0.01 , and in the *ApoE3* group, it was 1.47 ± 0.01 ($P < .001$, unpaired t test) (Figure 5C). These results suggest that a reduced LTP occurs in 4-month-old *ApoE4* mouse hippocampus at the beginning of induction and is maintained afterward.

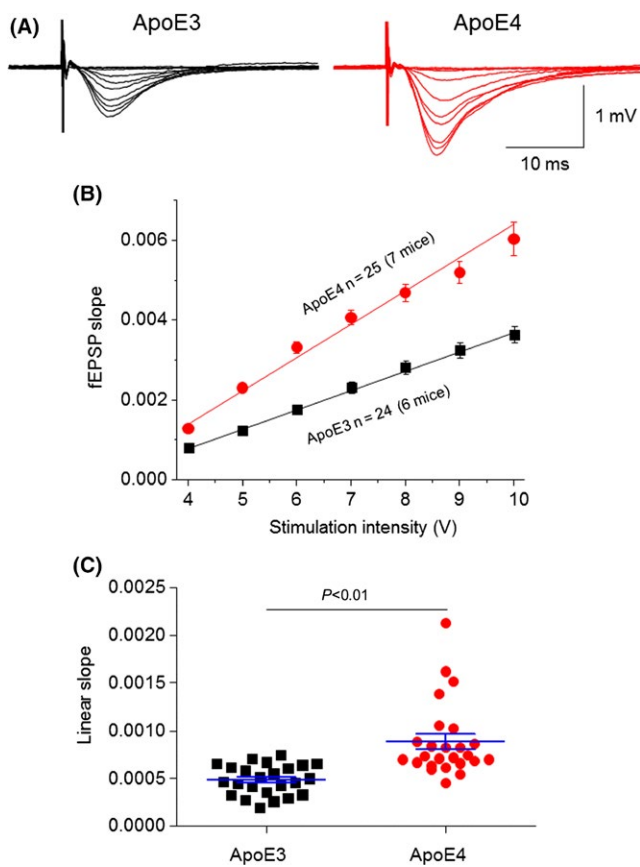


FIGURE 3 Comparison of input-output relationship curves between *ApoE4* and *ApoE3* TG mice. (A) Representative traces of different stimulation intensity-induced fEPSPs in a hippocampal CA1 slice prepared from *ApoE3* (left) and *ApoE4* (right). (B) Superimposition of input-output relationship curves fitted by linear equation shows linear slopes of *ApoE3* (black, $n=24$ slices from six mice) and *ApoE4* (red, $n=25$ from seven mice) groups (stimuli range, 4–10 V). (C) Summary of individual linear slopes from *ApoE3* (black) and *ApoE4* (red) groups. Statistical analysis (unpaired Student *t* test) indicates the difference is significant ($P<.001$)

3.5 | Comparisons of synaptic function between young and aged *ApoE4* mice

Data above clearly demonstrated synaptic abnormalities in 4-month-old *ApoE* mice as indicated by the enhanced basic synaptic transmission and PPF but impaired LTP induction and maintenance. We thus compared these synaptic functions between young (4-month-old) and aged (12-month-old) *ApoE4* mice. Compared to young *ApoE4* mice, aged *ApoE4* mice showed a reduced basic synaptic transmission (Figure 6A). In 20 hippocampal slices from six aged mice, the mean linear slope between 4 and 10 V-induced responses was 0.49 ± 0.04 , while in 25 hippocampal slices from seven young mice tested, this slope was 0.89 ± 0.07 ($P<.001$, unpaired *t* test, Figure 6B). Aged *ApoE4* mice also exhibited a reduced PPF compared to young *ApoE4* mice tested at all four P1 and P2 intervals (Figure 6C). For LTP, although aged *ApoE4* mice did not show a difference in mean LTP induction (LTP 0–10 minutes) compared to young *ApoE4* mice (aged *ApoE4* = 1.34 ± 0.04 vs young *ApoE4* = 1.38 ± 0.02 , $P>.05$, Figure 6D),

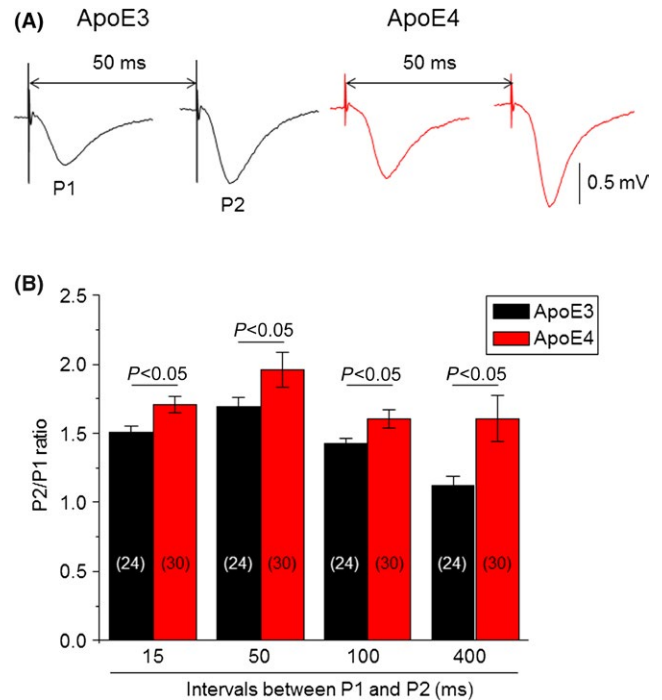


FIGURE 4 Comparison of paired-pulse facilitation between *ApoE4* and *ApoE3* transgenic mice. (A) Typical traces of fEPSP responses evoked by two stimuli at an interval of 50 ms from *ApoE3* (black) and *ApoE4* (red) mice. (B) Bar graph summarizing the P2/P1 ratios evoked by different paired-pulse stimulation intervals (15, 50, 100, and 400 ms) from *ApoE3* (black, $n=24$ from six mice) and *ApoE4* (red, $n=30$ from seven mice). The vertical bars represent \pm SE. The number inside each column indicates the number of slices tested. Statistical analysis using unpaired Student *t* test between *ApoE3* and *ApoE4* mice in different paired-pulse interval groups shows $P<.05$

the LTP maintenance (after LTP 50–60 minutes) was significantly reduced (aged *ApoE4* = 1.20 ± 0.006 vs young *ApoE4* = 1.31 ± 0.007 , $P<.0001$, Figure 6E). Collectively, these results suggest that the *ApoE4* genotype affects hippocampal synaptic transmission, PPF, and LTP in an age-dependent manner.

3.6 | Theta oscillations in hippocampal slices prepared from young *ApoE4* and *ApoE3* mice

Hippocampal theta oscillations represent the “online” state of the hippocampus and this rhythm is believed to be critical for temporal coding/decoding of active neuronal ensembles and the modification of synaptic weights.⁵³ In these experiments, we compared carbachol (CCh)-induced theta oscillations between young *ApoE4* and *ApoE3* mice using a field potential recording method, described in our previous report.^{22,48} Continuous bath perfusion of $50\text{-}\mu\text{mol L}^{-1}$ CCh to hippocampal slices induced impaired theta oscillations in *ApoE4* slices compared to *ApoE3* hippocampal slices (Figure 7A,B). To analyze these theta oscillations, we measured the theta-burst event-initiation time; total theta-burst event numbers during a 20-minute recording; and each theta-burst duration, frequency, and amplitude. As shown in Figure 7C, *ApoE4* mice were slower in initiation and had fewer burst events than *ApoE3* mice.

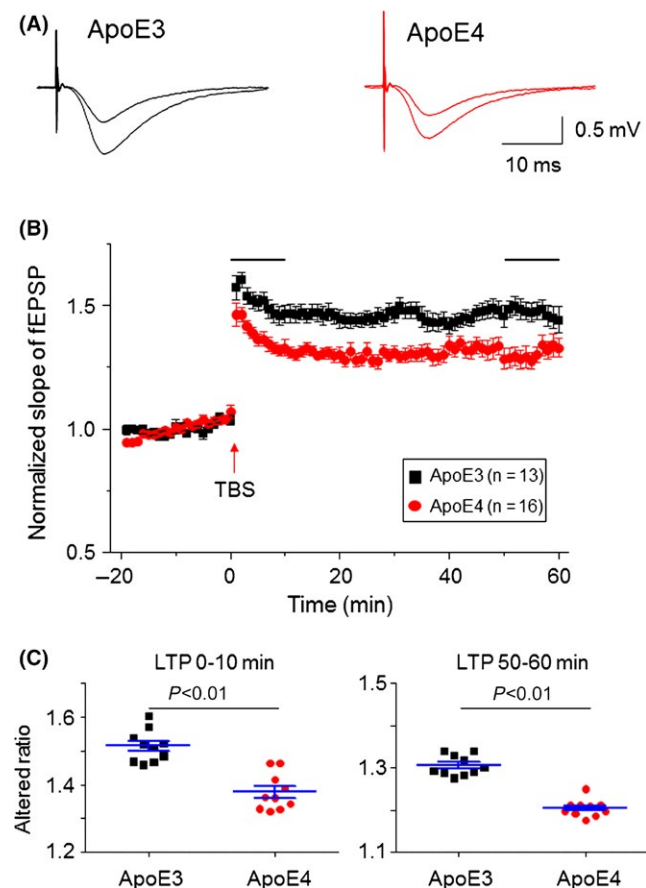


FIGURE 5 Comparison of hippocampal CA3-CA1 synaptic LTP between *ApoE4* and *ApoE3* transgenic mice. (A) Typical fEPSPs recorded before and after theta-burst tetanic stimulation from *ApoE3* and *ApoE4* mice. (B) Summary of hippocampal CA1 LTP from *ApoE3* (black, $n=13$ slices from six mice) and *ApoE4* (red, $n=16$ slices from seven mice). Theta-burst stimulations are indicated by horizontal lines above the fEPSP responses. (C) Comparison between *ApoE3* and *ApoE4* groups for LTP induction (after tetanic stimulation 1-10 min) and maintenance (after tetanic stimulation 50-60 min) demonstrate the impaired LTP induction and maintenance in *ApoE4* mice compared to *ApoE3* mice. TBS, theta-burst stimulation

3.7 | Hippocampal synaptic vesicle recycling in young *ApoE4* and *ApoE3* mice

It has been reported that *ApoE4* mice showed impaired presynaptic vesicle recycling.³² To compare hippocampal synaptic vesicle recycling in young *ApoE4* and *ApoE3* mice, we applied sustained electrical stimulations at the Schaffer collaterals pathway (5, 10, or 40 Hz for 4 seconds) similar to previously reported methods.⁵⁴ Figures 8A-C represent typical traces of 4, 10, and 40 Hz stimulation-induced fEPSP responses, respectively, in an *ApoE4* slice. A comparison of the ratio of last and first stimulation-induced fEPSPs (Figure 8D) and the ratio of maximal and first peak responses (Figure 8E) demonstrated no significant difference between *ApoE4* ($n=10$) and *ApoE3* ($n=8$) mice in three stimulatory parameters (5, 10, and 40 Hz). These results showed no significant changes in hippocampal CA1 vesicle recycling in young *ApoE4* mice.

4 | DISCUSSION

The major findings of this study are that synaptic abnormalities in the hippocampus occur as early as 4 months in *ApoE4* mice. Morphologically, hippocampal pyramidal neurons had reduced dendritic length and branch numbers, as well as decreased spine density in these young *ApoE4* mice compared to *ApoE3* mice. Functionally, these neurons demonstrated enhanced CA3-CA1 basal synaptic transmission, enhanced PPF, but reduced LTP induction and maintenance. In addition, young *ApoE4* mice also showed impaired carbachol-induced hippocampal theta oscillations without changes in synaptic vesicle recycling. Taken together, our study provides direct experimental evidence that young *ApoE4* mice exhibit morphologically and functionally impaired synapses in hippocampal CA1 neurons. This will help us to understand the impact of *ApoE4* in synaptic function, in animal learning behaviors, as well as in learning and memory of young adults.

4.1 | Young *ApoE4* mice show abnormalities in hippocampal CA1 neuronal dendritic morphology and spine density

Previous studies have demonstrated a morphological alteration in the hippocampus in *ApoE4* mice, including reduced levels of the presynaptic glutamatergic transporter, VGluT, in CA3, CA1, and DG hippocampal neurons of 4-month-old *ApoE4* mice compared to *ApoE3* mice.³⁸ However, the corresponding inhibitory GABAergic nerve terminals were not affected by the *ApoE* genotype,³⁸ although a significant change of GABAergic terminals occurred in aged *ApoE4* mice.⁵⁵ These findings suggest that the alterations in glutamatergic synaptic morphology and function are early pathological markers in *ApoE4* mice. In addition, decreased levels of cortical, but not hippocampal, neuronal spines⁵³; postsynaptic glutamate receptors³²; and the scaffold protein PSD-95²⁹ have been reported in *ApoE4* mice. These data suggest that the *ApoE4* genotype affects neuronal dendritic morphology and synaptic spine density.⁴³ In the present study, we demonstrated that, compared to 4-month-old *ApoE3* mice, hippocampal CA1 pyramidal neurons from age-matched *ApoE4* mice showed significant reductions in dendritic length and spine density. Our results are consistent with previous reports that young (4-month-old) *ApoE4* mice show significant changes in synaptic morphology and glutamate transporter.³⁸ However, our results are different from the report of Dumanis et al.⁵³ in which there were no significant alterations in hippocampal dendritic spine density between 1-, 3- and 12-month-old *ApoE4* mice using Golgi staining. The difference in findings may be explained by the variation in experimental approach as Golgi staining tends to underestimate spine density.^{56,57} Using Imaris reconstruction following confocal Z-stack, we were able to quantify accurately the dendritic spines on the Z plane, which is not possible in the Golgi-stained sections. Our approach (biocytin injection followed by avidin-Alexa 488) also minimizes the tissue shrinkage that is inevitable in Golgi stain section. Therefore, the spine density using these two approaches may not be readily comparable. Collectively, we demonstrated abnormalities of dendritic morphology and spine density in young *ApoE4* mice, which

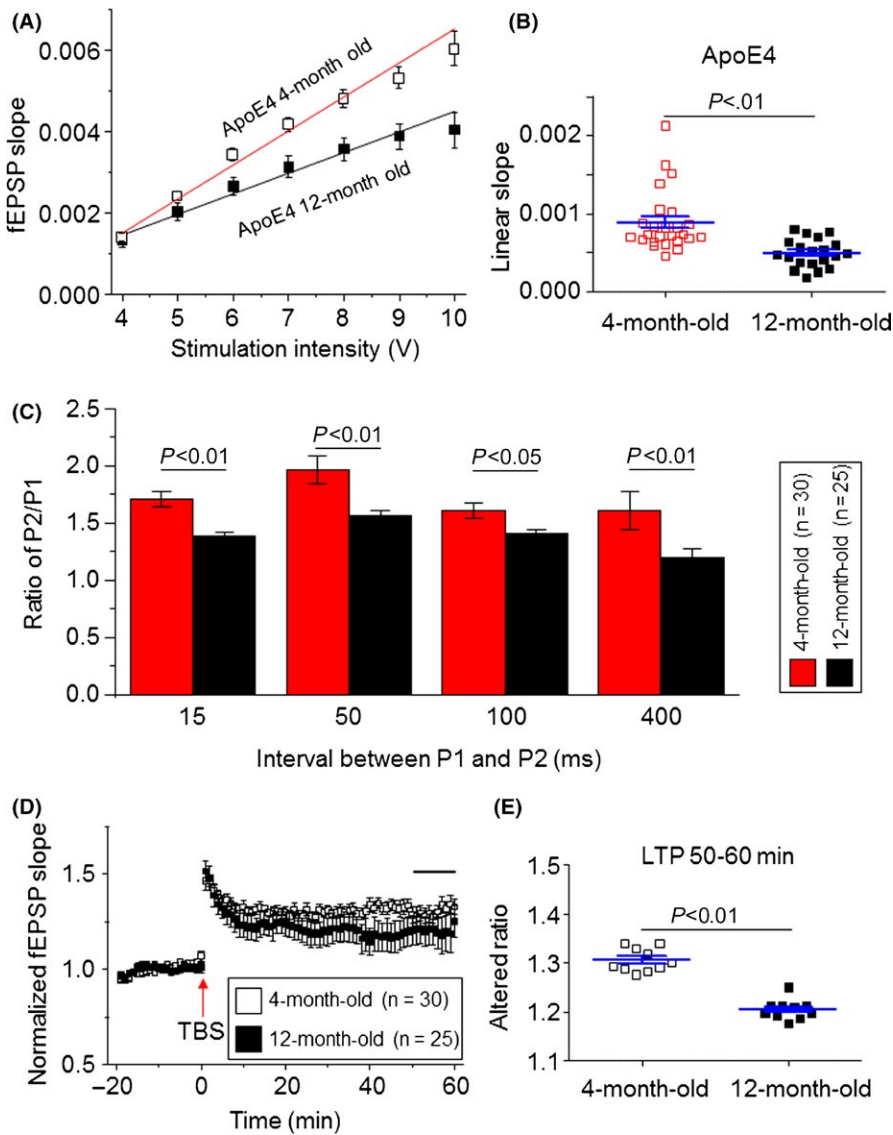


FIGURE 6 Comparison of synaptic functions between 4- and 12-month-old *ApoE4* mice. (A) Representative input-output relationship curves from 4-month-old (open squares, $n=25$ from seven mice, the same data from Figure 3B) and 12-month-old *ApoE4* (filled squares, $n=20$ slices from seven mice) groups. (B) Statistical comparison of linear slopes of each linear fit individual input-output relationship curve from 4-month-old (open squares) and 12-month-old (filled squares) *ApoE4* groups ($P<0.01$). (C) Bar chart shows comparison of P2/P1 ratios at different stimulation intervals between 4-month-old (white, $n=30$ slices from 14 mice) and 12-month-old (black, $n=25$ slices from seven mice) *ApoE4* mice. (D) Comparison of hippocampal CA1 LTP between 4- ($n=30$ from 14 mice) and 12-month-old ($n=20$ slices from six mice) *ApoE4* mice. (E) Statistical comparison of LTP maintenance (after tetanic stimulation 50-60 min) between 4- and 12-month-old *ApoE4* mice ($P<0.01$)

suggests an important basis for hippocampal synaptic functional deficits or even animal behavioral alterations.

4.2 | Young *ApoE4* mice show hippocampal synaptic functional abnormalities

We systemically examined the synaptic function of the hippocampus in young *ApoE4* mice using electrophysiological recordings of brain slices, and compared these to the age-matched *ApoE3* mice because *ApoE3* mice suffered the same transgenic process and showed no synaptic abnormality compared to wild type mice (Fig. S1). We choose mice of this age because hippocampal synaptic deficits have already been reported in aged *ApoE4* mice.⁴⁰ Previous studies in 4-month-old *ApoE4* mice have found the reduced hippocampal presynaptic glutamatergic vesicles (VGLut1) and postsynaptic synaptic protein (PD95), as well as animal learning behaviors.^{38,39} However, in addition to these protein expression and behavioral changes, it remains unclear whether hippocampal synaptic function is altered. Thus, our study sought to fill this knowledge gap. As expected, we found a significant

reduction in theta-burst tetanic stimulation-induced LTP in CA3-CA1 synapses. The mechanisms underlying these synaptic alterations are still unclear. Based on our data and previous reports, the *ApoE* gene affects both presynaptic and postsynaptic functions. Presynaptically, *ApoE4* mice exhibit the reduced glutamatergic vesicles (VGLut1)³⁸ and glutamate release probability (shown enhanced PPF ratio in Figure 4). Postsynaptically, *ApoE4* mice show the reduced postsynaptic synaptic protein (PD95)³⁹ and hippocampal dendritic morphology abnormalities (Figures 1,2) and LTP deficit (Figure 5). These lines of evidence suggest a net deficit in synaptic transmission of *ApoE4* hippocampal CA3-CA1. It is intriguing to observe an enhanced hippocampal neuronal excitability (left shift of I-O curve) in 4-month-old *ApoE4* mice compared to age-matched *ApoE3* mice. We postulate that this change may reflect a functional compensation at an early stage of brain development in *ApoE4* mice to overcome the synaptic and dendritic morphological abnormality and presynaptic glutamatergic vesicle deficit.³⁸ Our findings are both consistent with and different from previous reports for various potential reasons. First is the mouse age. It has been well accepted that the *APOE4* gene affects cognitive function and learning

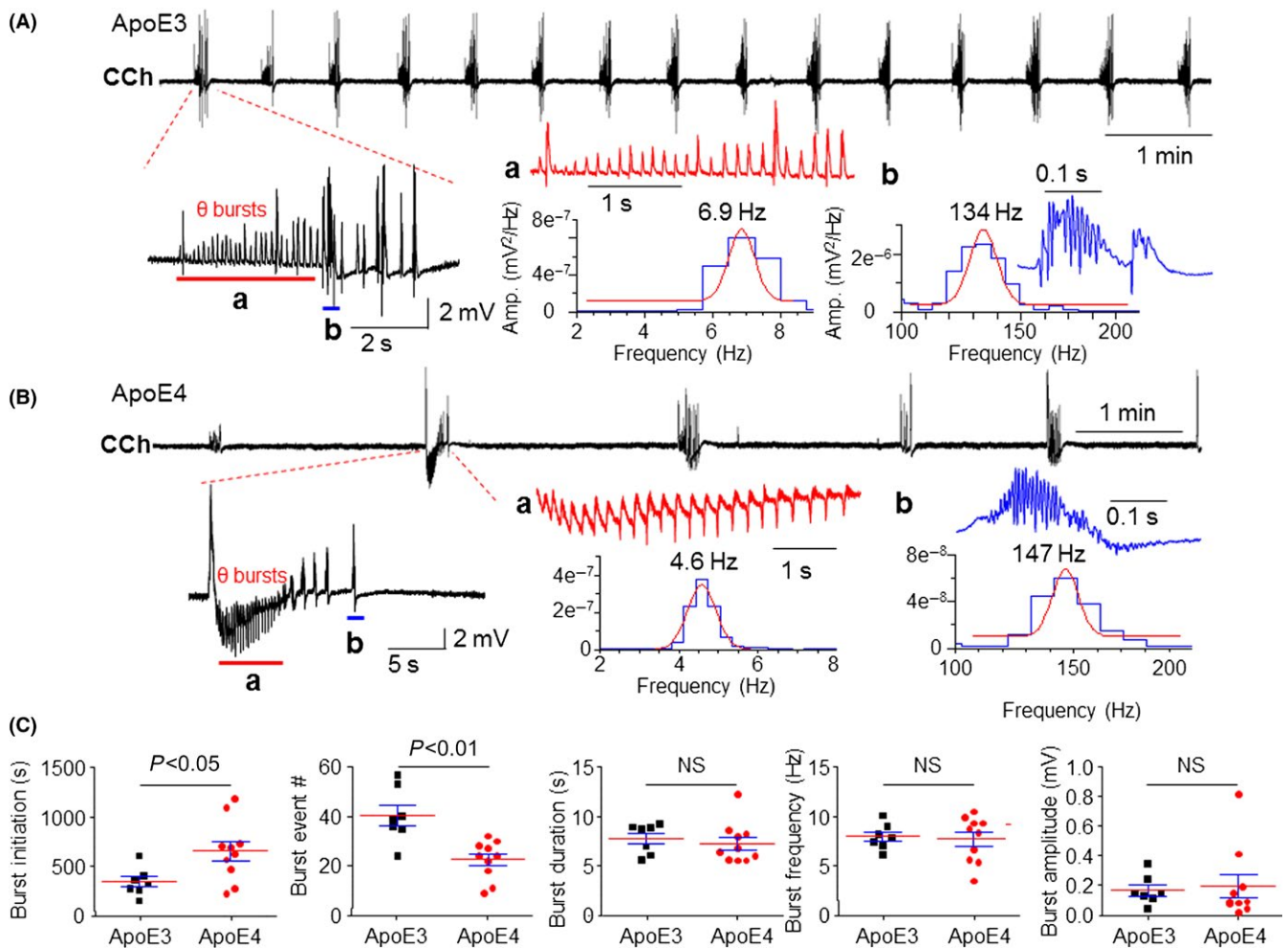


FIGURE 7 Comparison of CCh-induced theta oscillations in hippocampal slices prepared from *ApoE4* and *ApoE3* mice. Typical traces of bath perfusion of $50 \mu\text{mol L}^{-1}$ CCh-induced theta oscillations recorded in hippocampal CA1 area from *ApoE3* (A) and *ApoE4* mice (B) represent repetitive burst events during a 10-min recording period. The expanded timescales on the left show two components of bursts, theta rhythm (indicated by red bar) and lower frequency spikes (blue bar). The further expanded timescales on the right show theta oscillations (red, 4–9 Hz) and high-frequency oscillations (blue, >100 Hz). (C) Statistical analysis shows that *ApoE4* mice had significant impairment of CCh-induced theta oscillations including a prolonged initiation time of burst events ($P < .05$) and reduced burst event numbers ($P < .01$). NS, not significant

and memory in an age-dependent manner.^{58–60} For example, different changes in hippocampal LTP in different ages of *ApoE4* mice have been noted: in 2-month-old mice, hippocampal LTP was enhanced⁴² or had no change,³² but in 24- to 27-month-old mice, hippocampal LTP was impaired.⁴⁰ We showed here that in 4-month-old *ApoE4* mice, hippocampal LTP induction and maintenance were already reduced compared to 4-month-old *ApoE3* mice. The finding of lower hippocampal synaptic LTP in 4-month-old *ApoE4* mice is well supported by previous reports that 4-month-old *ApoE4* mice showed reduced levels of the presynaptic glutamatergic vesicular transporter (VGLUT)³⁸ and impaired hippocampus-related learning and memory tasks.³⁹ The second reason for the difference between our results and other published studies is due to the method of LTP induction. In 2-month-old *ApoE4* mice, hippocampal CA1 LTP was induced by high-frequency tetanic stimulation (100 Hz for 1 seconds)⁴² When using similarly aged (2-month-old) *ApoE4* mice, theta-burst tetanic stimulation-induced LTP showed no

change between *ApoE4* and *ApoE3* mice.³² The third reason is related to the area of brain investigated. Using high-frequency tetanic stimulation in young *ApoE4* mice, hippocampal CA1 LTP was enhanced in CA3–CA1 area⁴² while hippocampal dentate gyrus LTP was reduced compared to age-matched *ApoE3* mice.⁶¹ Collectively, these data suggest that there are several factors such as animal ages, LTP induction protocols, and brain areas that studies contributing to hippocampal synaptic plasticity in *ApoE4* mice. Thus, caution is needed when analyzing and interpreting these data.

4.3 | Young *ApoE4* mice exhibit impaired hippocampal theta oscillations

The key role of the hippocampus for intact episodic memory has been firmly established by neuropsychological studies, animal models, computational models, and human neuroimaging.⁶² The hippocampus has

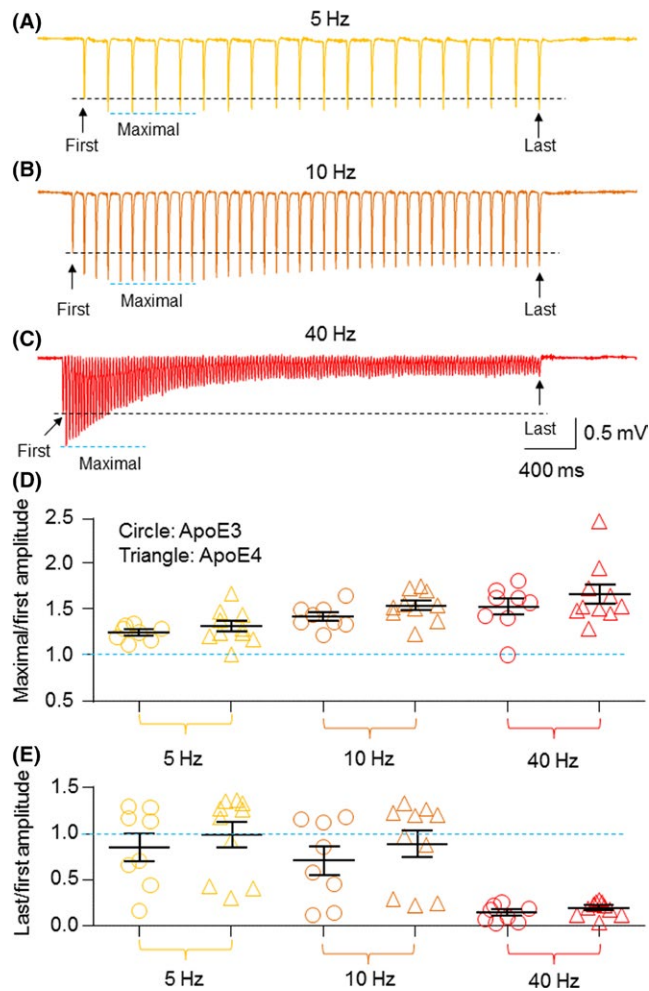


FIGURE 8 Comparison of fEPSP evoked by sustained stimulations (5, 10, and 40 Hz for 4 s) between *ApoE4* and *ApoE3* transgenic mice. Evoked fEPSPs in a hippocampal slice from 4-month-old *ApoE4* mice were elicited by a sustained stimulation with 50% maximal stimulation intensity at 5 Hz (A), 10 Hz (B), or 40 Hz (C) for 4 s. (D) Graph summarizes the ratios of maximal fEPSP slope/first fEPSP slope by 5, 10, or 40 Hz stimulations from the *ApoE3* and *ApoE4* groups. (E) Graph summarizes the ratios of last fEPSP slope/first fEPSP slope by 5, 10, or 40 Hz stimulations from the *ApoE3* and *ApoE4* groups

three types of rhythmic activity: theta (4–12 Hz), beta (13–30 Hz), and gamma (30–80 Hz). These activities reflect different states of the brain and behaviors.⁶³ The theta oscillations represent the “online” state of the hippocampus. The extracellular currents underlying theta waves are generated mainly by the entorhinal input, CA3 (Schaffer) collaterals, and voltage-dependent Ca^{2+} currents in pyramidal cell dendrites. The rhythm is believed to be critical for temporal coding/decoding of active neuronal ensembles and the modification of synaptic weights.⁶⁴ Hippocampal neuronal network oscillations are associated with attention, learning, and memory and are impaired in disease conditions such as AD. Recently, aged *ApoE4* mice were reported to have fewer slow-wave responses than *ApoE3* mice and significantly reduced slow gamma oscillations during sharp-wave ripples, which critically contributes to *ApoE4*-mediated learning and memory impairments.⁶⁰

Furthermore, a significant reduction in hippocampal dentate gyrus GABAergic interneurons has been found in aged *ApoE4* mice. Because the GABAergic neurons were not abnormal in young (3–4 months old) *ApoE4* mice,³⁸ we did not examine hippocampal gamma oscillations in young *ApoE4* mice. Instead, we focused on hippocampal cholinergic theta oscillations in young *ApoE4* mice. We found significant alterations in CCh ($50 \mu\text{mol L}^{-1}$)-induced theta oscillation initial time and burst event numbers in young *ApoE4* transgenic mice compared to the age-matched *ApoE3* transgenic mice. Collectively, these data provide the first evidence of possible neuronal mechanisms of learning behavioral deficits in 4-month-old *ApoE4* mice.

5 | CONCLUSION

Synaptic morphology and function abnormalities in the hippocampus occur as early as 4 months in *ApoE4* mice. In addition, young *ApoE4* mice also exhibit impaired carbachol-induced hippocampal theta oscillations without changes in synaptic vesicle recycling. Therefore, this study provides direct experimental evidence that will help us to understand the impact of *ApoE4* in synaptic function, in animal learning behaviors, as well as in learning and memory of young adults.

ACKNOWLEDGMENTS

This study was funded by the Arizona Alzheimer’s Disease Consortium (JS), Barrow Neurological Foundation (JW), the National Science Foundation of China (81671050 to JS), and the Program for High-level Talent Fund of Hebei Province of China (No. A201401041 to GS).

CONFLICT OF INTEREST

The authors declare no conflict of interest.

REFERENCES

- Masters CL, Simms G, Weinman NA, Multhaup G, McDonald BL, Beyreuther K. Amyloid plaque core protein in Alzheimer disease and Down syndrome. *Proc Natl Acad Sci USA*. 1985; 82:4245–4249.
- Tesseur I, Zou K, Esposito L, et al. Deficiency in neuronal TGF- β signaling promotes neurodegeneration and Alzheimer’s pathology. *J Clin Invest*. 2006;116:3060–3069.
- Bloom GS. Amyloid- β and tau: the trigger and bullet in Alzheimer disease pathogenesis. *JAMA Neurol*. 2014;71:505–508.
- Crimins JL, Pooler A, Polydoro M, Luebke JI, Spires-Jones TL. The intersection of amyloid β and tau in glutamatergic synaptic dysfunction and collapse in Alzheimer’s disease. *Ageing Res Rev*. 2013;12:757–763.
- Pozueta J, Lefort R, Shelanski ML. Synaptic changes in Alzheimer’s disease and its models. *Neuroscience*. 2013;251:51–65.
- Ingelsson M, Fukumoto H, Newell KL, et al. Early A β accumulation and progressive synaptic loss, gliosis, and tangle formation in AD brain. *Neurology*. 2004;62:925–931.
- Braak H, Braak E. Neuropathological staging of Alzheimer-related changes. *Acta Neuropathol*. 1991;82:239–259.
- Fjell AM, Walhovd KB. Neuroimaging results impose new views on Alzheimer’s disease—the role of amyloid revisited. *Mol Neurobiol*. 2012;45:153–172.

9. Jack CR Jr, Knopman DS, Jagust WJ, et al. Hypothetical model of dynamic biomarkers of the Alzheimer's pathological cascade. *Lancet Neurol.* 2010;9:119-128.
10. Rusinek H, De Santi S, Frid D, et al. Regional brain atrophy rate predicts future cognitive decline: 6-year longitudinal MR imaging study of normal aging. *Radiology.* 2003;229:691-696.
11. Carmichael O, Schwarz C, Drucker D, et al. Longitudinal changes in white matter disease and cognition in the first year of the Alzheimer disease neuroimaging initiative. *Arch Neurol.* 2010;67:1370-1378.
12. Mosconi L, Berti V, Glodzik L, Pupi A, De Santi S, de Leon MJ. Pre-clinical detection of Alzheimer's disease using FDG-PET, with or without amyloid imaging. *J Alzheimers Dis.* 2010;20:843-854.
13. Frisoni GB, Giannakopoulos P. The specificity of amyloid imaging in the diagnosis of neurodegenerative diseases. *Neurobiol Aging.* 2012;33:1021-1022.
14. Briggs CA, Chakroborty S, Stutzmann GE. Emerging pathways driving early synaptic pathology in Alzheimer's disease. *Biochem Biophys Res Commun.* 2017;483:988-997.
15. Masliah E. Mechanisms of synaptic pathology in Alzheimer's disease. *J Neural Transm Suppl.* 1998;53:147-158.
16. Conforti L, Adalbert R, Coleman MP. Neuronal death: where does the end begin? *Trends Neurosci.* 2007;30:159-166.
17. Saunders AM, Strittmatter WJ, Schmechel D, et al. Association of apolipoprotein E allele epsilon 4 with late-onset familial and sporadic Alzheimer's disease. *Neurology.* 1993;43:1467-1472.
18. Saunders AM, Schmechel D, Breitner JC, et al. Apolipoprotein E epsilon 4 allele distributions in late-onset Alzheimer's disease and in other amyloid-forming diseases. *Lancet.* 1993;342:710-711.
19. Corder EH, Saunders AM, Strittmatter WJ, et al. Gene dose of apolipoprotein E type 4 allele and the risk of Alzheimer's disease in late onset families. *Science.* 1993;261:921-923.
20. Roses AD. Apolipoprotein E and Alzheimer's disease. A rapidly expanding field with medical and epidemiological consequences. *Ann N Y Acad Sci.* 1996;802:50-57.
21. Liu CC, Kanekiyo T, Xu H, Bu G. Apolipoprotein E and Alzheimer disease: risk, mechanisms and therapy. *Nat Rev Neurol.* 2013;9:106-118.
22. Kim J, Basak JM, Holtzman DM. The role of apolipoprotein E in Alzheimer's disease. *Neuron.* 2009;63:287-303.
23. Schmechel DE, Saunders AM, Strittmatter WJ, et al. Increased amyloid beta-peptide deposition in cerebral cortex as a consequence of apolipoprotein E genotype in late-onset Alzheimer disease. *Proc Natl Acad Sci USA.* 1993;90:9649-9653.
24. Strittmatter WJ, Saunders AM, Schmechel D, et al. Apolipoprotein E: high-avidity binding to beta-amyloid and increased frequency of type 4 allele in late-onset familial Alzheimer disease. *Proc Natl Acad Sci USA.* 1993;90:1977-1981.
25. Strittmatter WJ, Saunders AM, Goedert M, et al. Isoform-specific interactions of apolipoprotein E with microtubule-associated protein tau: implications for Alzheimer disease. *Proc Natl Acad Sci USA.* 1994;91:11183-11186.
26. Sunderland T, Mirza N, Putnam KT, et al. Cerebrospinal fluid beta-amyloid1-42 and tau in control subjects at risk for Alzheimer's disease: the effect of APOE epsilon4 allele. *Biol Psychiatry.* 2004;56:670-676.
27. Nwabuisi-Heath E, Rebeck GW, Ladu MJ, Yu C. ApoE4 delays dendritic spine formation during neuron development and accelerates loss of mature spines in vitro. *ASN Neuro.* 2014;6:e00134.
28. Dumanis SB, DiBattista AM, Miessau M, Moussa CE, Rebeck GW. APOE genotype affects the pre-synaptic compartment of glutamatergic nerve terminals. *J Neurochem.* 2013;124:4-14.
29. Zhu Y, Nwabuisi-Heath E, Dumanis SB, et al. APOE genotype alters glial activation and loss of synaptic markers in mice. *Glia.* 2012;60:559-569.
30. Arendt T, Schindler C, Bruckner MK, et al. Plastic neuronal remodeling is impaired in patients with Alzheimer's disease carrying apolipoprotein epsilon 4 allele. *J Neurosci.* 1997;17:516-529.
31. White F, Nicoll JA, Roses AD, Horsburgh K. Impaired neuronal plasticity in transgenic mice expressing human apolipoprotein E4 compared to E3 in a model of entorhinal cortex lesion. *Neurobiol Dis.* 2001;8:611-625.
32. Chen Y, Durakoglugil MS, Xian X, Herz J. ApoE4 reduces glutamate receptor function and synaptic plasticity by selectively impairing ApoE receptor recycling. *Proc Natl Acad Sci USA.* 2010;107:12011-12016.
33. Kim J, Yoon H, Basak J, Kim J. Apolipoprotein E in synaptic plasticity and Alzheimer's disease: potential cellular and molecular mechanisms. *Mol Cells.* 2014;37:767-776.
34. Reiman EM, Chen K, Liu X, et al. Fibrillar amyloid-beta burden in cognitively normal people at 3 levels of genetic risk for Alzheimer's disease. *Proc Natl Acad Sci USA.* 2009;106:6820-6825.
35. Heise V, Filippini N, Ebmeier KP, Mackay CE. The APOE varepsilon4 allele modulates brain white matter integrity in healthy adults. *Mol Psychiatry.* 2011;16:908-916.
36. Caselli RJ, Dueck AC, Osborne D, et al. Longitudinal modeling of age-related memory decline and the APOE epsilon4 effect. *N Engl J Med.* 2009;361:255-263.
37. Dean DC 3rd, Jerskey BA, Chen K, et al. Brain differences in infants at differential genetic risk for late-onset Alzheimer disease: a cross-sectional imaging study. *JAMA Neurol.* 2014;71:11-22.
38. Liraz O, Boehm-Cagan A, Michaelson DM. ApoE4 induces Abeta42, tau, and neuronal pathology in the hippocampus of young targeted replacement apoE4 mice. *Mol Neurodegener.* 2013;8:16.
39. Salomon-Zimri S, Boehm-Cagan A, Liraz O, Michaelson DM. Hippocampus-related cognitive impairments in young apoE4 targeted replacement mice. *Neurodegener Dis.* 2014;13:86-92.
40. Yun SH, Park KA, Kwon S, et al. Estradiol enhances long term potentiation in hippocampal slices from aged apoE4-TR mice. *Hippocampus.* 2007;17:1153-1157.
41. Qiao F, Gao XP, Yuan L, Cai HY, Qi JS. Apolipoprotein E4 impairs in vivo hippocampal long-term synaptic plasticity by reducing the phosphorylation of CaMKIIalpha and CREB. *J Alzheimers Dis.* 2014;41:1165-1176.
42. Kitamura HW, Hamanaka H, Watanabe M, et al. Age-dependent enhancement of hippocampal long-term potentiation in knock-in mice expressing human apolipoprotein E4 instead of mouse apolipoprotein E. *Neurosci Lett.* 2004;369:173-178.
43. Ji Y, Gong Y, Gan W, Beach T, Holtzman DM, Wisniewski T. Apolipoprotein E isoform-specific regulation of dendritic spine morphology in apolipoprotein E transgenic mice and Alzheimer's disease patients. *Neuroscience.* 2003;122:305-315.
44. Hartman RE, Wozniak DF, Nardi A, Olney JW, Sartorius L, Holtzman DM. Behavioral phenotyping of GFAP-*apoE3* and -*apoE4* transgenic mice: *apoE4* mice show profound working memory impairments in the absence of Alzheimer's-like neuropathology. *Exp Neurol.* 2001;170:326-344.
45. Knouff C, Hinsdale ME, Mezdour H, et al. Apo E structure determines VLDL clearance and atherosclerosis risk in mice. *J Clin Invest.* 1999;103:1579-1586.
46. Wu J, Fisher RS. Hyperthermic spreading depressions in the immature rat hippocampal slice. *J Neurophysiol.* 2000;84:1355-1360.
47. Song C, Murray TA, Kimura R, et al. Role of alpha7-nicotinic acetylcholine receptors in tetanic stimulation-induced gamma oscillations in rat hippocampal slices. *Neuropharmacology.* 2005;48:869-880.
48. Kimura R, Ma LY, Wu C, et al. Acute exposure to the mitochondrial complex I toxin rotenone impairs synaptic long-term potentiation in rat hippocampal slices. *CNS Neurosci Ther.* 2012;18:641-646.
49. Qiu S, Lu Z, Levitt P. MET receptor tyrosine kinase controls dendritic complexity, spine morphogenesis, and glutamatergic synapse maturation in the hippocampus. *J Neurosci.* 2014;34:16166-16179.
50. Sholl DA. Dendritic organization in the neurons of the visual and motor cortices of the cat. *J Anat.* 1953;87:387-406.

51. Lippman J, Dunaevsky A. Dendritic spine morphogenesis and plasticity. *J Neurobiol.* 2005;64:47-57.
52. Zucker RS, Regehr WG. Short-term synaptic plasticity. *Annu Rev Physiol.* 2002;64:355-405.
53. Dumanis SB, Tesoriero JA, Babus LW, et al. ApoE4 decreases spine density and dendritic complexity in cortical neurons in vivo. *J Neurosci.* 2009;29:15317-15322.
54. Qiu X, Zhu Q, Sun J. Quantitative analysis of vesicle recycling at the calyx of Held synapse. *Proc Natl Acad Sci USA.* 2015;112:4779-4784.
55. Andrews-Zwilling Y, Bien-Ly N, Xu Q, et al. Apolipoprotein E4 causes age- and Tau-dependent impairment of GABAergic interneurons, leading to learning and memory deficits in mice. *J Neurosci.* 2010;30:13707-13717.
56. Shen H, Sesack SR, Toda S, Kalivas PW. Automated quantification of dendritic spine density and spine head diameter in medium spiny neurons of the nucleus accumbens. *Brain Struct Funct.* 2008;213:149-157.
57. Asadi M, Rokni-Yazdi H, Salehinia F, Allameh FS. Metastatic renal cell carcinoma initially presented with an intramedullary spinal cord lesion: a case report. *Cases J.* 2009;2:7805.
58. Tang X, Holland D, Dale AM, Miller MI. Alzheimer's Disease Neuroimaging I. APOE affects the volume and shape of the amygdala and the hippocampus in mild cognitive impairment and Alzheimer's Disease: age matters. *J Alzheimers Dis.* 2015;47:645-660.
59. Thai C, Lim YY, Villemagne VL, et al. Amyloid-related memory decline in preclinical Alzheimer's disease is dependent on apoe epsilon4 and is detectable over 18-months. *PLoS ONE.* 2015;10:e0139082.
60. Gillespie AK, Jones EA, Lin YH, et al. Apolipoprotein e4 causes age-dependent disruption of slow gamma oscillations during hippocampal sharp-wave ripples. *Neuron.* 2016;90:740-751.
61. Trommer BL, Shah C, Yun SH, et al. ApoE isoform affects LTP in human targeted replacement mice. *NeuroReport.* 2004;15:2655-2658.
62. Sauvage MM, Fortin NJ, Owens CB, Yonelinas AP, Eichenbaum H. Recognition memory: opposite effects of hippocampal damage on recollection and familiarity. *Nat Neurosci.* 2008;11:16-18.
63. Buzsaki G, Wang XJ. Mechanisms of gamma oscillations. *Annu Rev Neurosci.* 2012;35:203-225.
64. Buzsaki G. Theta oscillations in the hippocampus. *Neuron.* 2002;33:325-340.

SUPPORTING INFORMATION

Additional Supporting Information may be found online in the supporting information tab for this article.

How to cite this article: Sun G-Z, He Y-C, Ma X-K, et al. Hippocampal synaptic and neural network deficits in young mice carrying the human APOE4 gene. *CNS Neurosci Ther.* 2017;23:748-758. <https://doi.org/10.1111/cns.12720>